# DIFFERENTIATION OF TUMOR TYPES IN VIVO BY SCATTERER PROPERTY ESTIMATES AND PARAMETRIC IMAGES USING ULTRASOUND BACKSCATTER

Michael L. Oelze[1], James F. Zachary[2] and William D. O'Brien Jr.[1,2]

[1]Department of Electrical and Computer Engineering, [2]Department of Bioengineering
University of Illinois at Urbana-Champaign

## ABSTRACT

Two kinds of solid tumors were acquired and scanned in vivo ultrasonically. The first tumor series consisted of spontaneous mammary tumors (fibroadenomas) in rats. The second tumor series were acquired by culturing a carcinoma cell line (4T1-MMT) in culture media. When the cell population reached 80 % confluence in the culture flask, the cells were injected into the fat pad of BALB/c mice. Subsequent carcinoma tumors were allowed to grow to about 1 cm in diameter. The scatterer properties of average scatterer diameter and acoustic concentration were estimated from a Gaussian form factor using the backscattered ultrasound measured from both kinds of tumors. An f/4 transducer (10-MHz center frequency, 8-MHz bandwidth) was used to scan both tumor types. An f/3 transducer (20-MHz center frequency, 16-MHz bandwidth) was also used to scan the carcinomas. Parametric images of the tumors were constructed utilizing the estimated scatterer properties for regions of interest inside the tumors. Differences between the two tumor types were clearly seen from the scatterer property estimates and the parametric images. The average scatterer diameter and acoustic concentration for the fibroadenomas were estimated to be 105 ± 25 μm and –15.6 ± 5 dB ($mm^{-3}$), respectively. The average scatterer diameter for the carcinomas was estimated to be 39.8 ± 12.4 μm with the 10-MHz transducer and 30 ± 9.6 μm with the 20-MHz transducer. The average acoustic concentration was estimated to be 21.3 ± 5.9 dB ($mm^{-3}$) with the 10-MHz transducer and 10.6 ± 6.9 dB ($mm^{-3}$) with the 20-MHz transducer. Differences between the 10-MHz and 20-MHz estimates were due to the utilization of a more optimal *ka* range with the 20-MHz transducer in the estimator. Light microscopic evaluations of the fibroadenomas showed cellular structures of around 100 μm in size, and carcinomas showed cell nuclei with an average size of approximately15 μm in diameter. The total cellular size can range from 50 % to 200 % larger than the nucleus size. Work supported by NIH F32 CA96419 to MLO and by the University of Illinois Research Board.

## I. INTRODUCTION

Conventional B-mode images of tissues using ultrasound are made by relating the envelope-detected RF signal backscattered from the tissues to a grayscale image. The frequency-dependent information contained in the backscattered RF signal is not utilized by conventional B-mode imaging. The frequency dependence has been hypothesized to contain information about tissue microstructure. Further examination of backscattered RF signals may yields means of characterizing and differentiating between types of tissues.

Models have been used to relate frequency-dependent backscatter from tissues to microstructure [1,2]. The models have allowed estimates of average scatterer properties (size, shape and acoustic concentration) of tissue microstructure from backscattered RF signals for purposes of detecting and classifying tissues [2,3,4]. Parametric images created from estimates have been used to classify tissues [3,4,5,6]. Classification of tissues through parametric imaging techniques may be medically significant to diagnosis and treat disease.

In this work, a parametric imaging technique based on scatterer property estimation is used to differentiate between a spontaneous fibroadenoma in rats and a 4T1 carcinoma mammary tumor in mice.

## II. THEORY

Gaussian scatterers have been used to model scattering from many soft tissues [6,7,8]. The theoretical power spectrum from a collection of Gaussian scatterers is, from Lizzi et al. [1],

$$W_{theor}(f) = \frac{185 L q^2 f^4 a_{eff}^6 n z_{rel}^2 e^{-12.59 f^2 a_{eff}^2}}{36\pi^4 \left[1 + 2.66\left(qfa_{eff}\right)^2\right]} \qquad (1)$$

where $L$ is the gate length, $f$ is frequency, $q$ is ratio of transducer radius to distance from the ROI, $nz_{rel}^2$ is acoustic concentration and $a_{eff}$ is the average effective radius of scatterers. Equation (1) takes into account the effects of the gating function (Hanning window) and transducer axial beam profile. The model assumes measurements are made in the depth of focus of a weakly focused transducer.

## III. EXPERIMENT

The experimental protocol was approved by campus Laboratory Animal Care Advisory Committee and satisfied all campus and National Institutes of Health rules for humane use of laboratory animals. Spontaneous mammary tumors (fibroadenomas) that had developed in eight Sprague-Dawley rats (Harlan, Indianapolis) were evaluated. 4T1 carcinoma cells were grown in culture medium and then transplanted into mice. Carcinoma tumors then developed in the mice at the site of injection. Each animal was euthanized and chest area was shaved on and around the tumor with electric clippers and depilated. Each animal was then placed on a holder in degassed water at 37° C for scanning.

Two single-element weakly focused transducers were used to scan laterally across the tumors. The first transducer had an aperture diameter of 12 mm and depth of focus of 22 mm. The center frequency of the transducer was 10 MHz with –6-dB pulse-echo bandwidth of 8 MHz. The second transducer had an aperture diameter of 6 mm and depth of focus ?? of 7 mm. The center frequency of the transducer was 20 MHz with –6-dB pulse-echo bandwidth of 16 MHz. Estimates of scatterer properties were made within the depth of focus of the transducers. The transducers were operated in pulse-echo mode through a Panametrics 5900 pulser/receiver (Waltham, MA). The signals were recorded and digitized on an oscilloscope (Lecroy 9354 TM; Chestnut Ridge, NY) and downloaded to a PC computer for post-processing. The sampling rate was 200 MHz. The transducer was moved laterally across the chest and tumor by a micropositioning system with step size of a ¼ beamwidth between each A-line scan. The assumed attenuation was 0.9 dB/cm/MHz in the rat fibroadenoma and 0.4 dB/cm/MHz in the carcinomas based on reports of attenuation measurements through chest walls and through tumor tissues [9].

Grey-scale B-mode images were constructed from the ultrasonic scans. ROIs were selected from the B-mode images and used to estimate the scattering parameters. The ROIs were boxes 3 mm on a side for the 10 MHz data and 1.5 mm on a side for the 20 MHz data. The ROIs corresponded to a sliding Hanning window with a 66% overlap. After making estimates from the power spectra from each ROI, parametric images were constructed for each animal. The parametric images took the two properties estimated from each ROI and related the estimates to a particular colored pixel. The pixels were then superimposed on the conventional B-mode images to form two parametric images per animal.

The measured power spectrum from an individual ROI consisted of the averaged power spectra from several A-lines. Frequency-dependent attenuation was compensated in the measured power spectrum. Including the attenuation-compensation function, $A(f)$, and averaging over the ROI yielded for the measured power spectrum

$$W_{meas}(f) = \frac{R^2}{4} A(f) \frac{\langle W_m(f) \rangle}{W_{ref}(f)} \qquad (6)$$

where $R$ is the reflection coefficient of the planar reflector in water. The planar reflector was used to obtain a calibration spectrum, $W_{ref}(f)$, to take out the effects of the equipment and settings on the measurement. The estimator used to obtain the

scatterer properties was the best-fit line estimator by Oelze et al. [3].

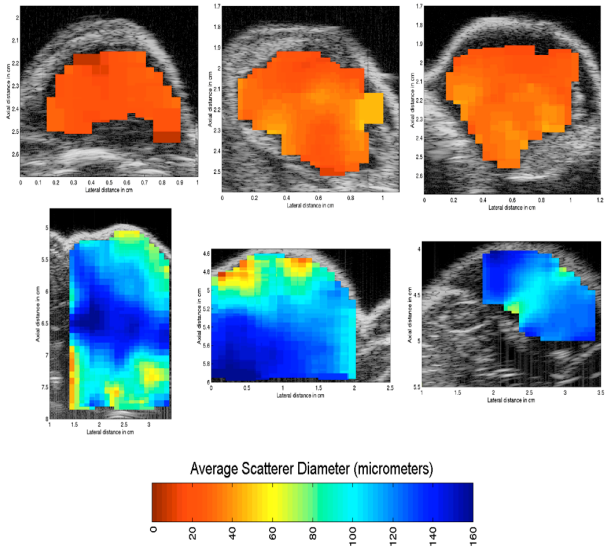


**Figure 1 Parametric images of carcinomas (top panel) and fibroadenoma (middle panel) using the estimated average scatterer size. The colorbar (bottom panel) relates the colored pixels to the scatter size.**

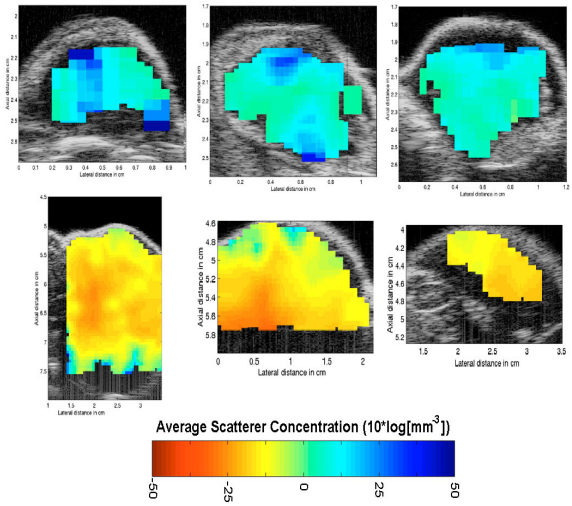


**Figure 2 Parametric images of carcinomas (top panel) and fibroadenoma (middle panel) using the estimated average acoustic concentration. The colorbar (bottom panel) relates the colored pixels to the acoustic concentration.**

Estimates of the average scatterer size and acoustic concentration can be seen in the parametric images of the tumors. Figure 1 shows the parametric images of the carcinomas and fibroadenomas using the estimated scatterer sizes. Figure 2 shows the parametric images of the carcinomas and fibroadenomas using the estimated acoustic concentrations.

The average scatterer diameter and acoustic concentration for the fibroadenomas were estimated to be 105 ± 25 μm and –15.6 ± 5 dB (mm$^{-3}$), respectively. The average scatterer diameter for the carcinomas was estimated to be 39.8 ± 12.4 μm with the 10-MHz transducer and 30 ± 9.6 μm with the 20-MHz transducer. The average acoustic concentration was estimated to be 21.3 ± 5.9 dB (mm$^{-3}$) with the 10-MHz transducer and 10.6 ± 6.9 dB (mm$^{-3}$) with the 20-MHz transducer.

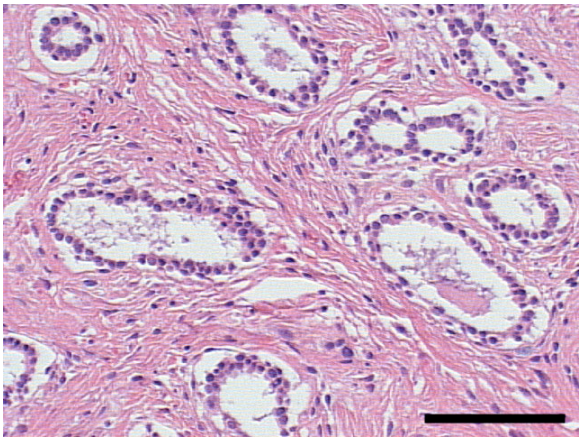

**(a)**

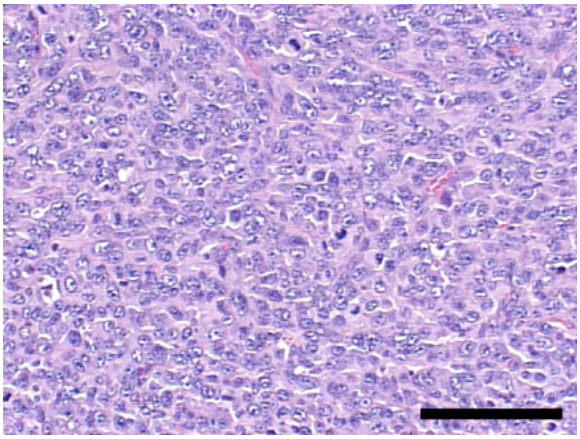

**(b)**

**Figure 3 Photomicrographs of fibroadenomas (a) and carcinomas (b). The black bar represents 100 μm.**

Differences between the 10-MHz and 20-MHz estimates were due to the utilization of a more optimal *ka* range with the 20-MHz transducer in the estimator. Light microscopic evaluations of the

fibroadenomas showed cellular structures of around 100 μm in size, and carcinomas showed cell nuclei with an average size of approximately15 μm in diameter. The total cellular size can range from 50% to 200% larger than the nucleus size. Figure 3 shows photomicrographs of the fibroadenoma and carcinoma tumors.

Comparison between the parametric images of the fibroadenomas and the carcinomas showed clear distinction. For the scatterer size images (figure 1) the carcinomas showed smaller scatterers than the fibroadenomas. The acoustic concentration images (figure2) showed that the carcinomas had a larger acoustic concentration than the fibroadenomas. A feature analysis plot of the estimated scatterer diameters versus acoustic concentrations is shown in Figure 4. The plot clearly shows a distinction between estimates of the two types of tumors.

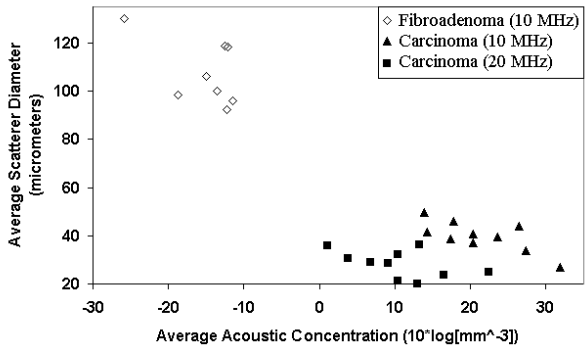


**Figure 4 Feature analysis plot of estimated scatterer properties for two types of tumors.**

## IV. CONCLUSION

An estimation technique was used to estimate average scatterer size and acoustic concentrations in two types of tumors. Parametric images were constructed incorporating the scatterer property estimates. Parametric images and scatterer property estimates clearly showed a distinction between the two types of tumors. Parametric imaging utilizing the scatterer property estimates may be useful in diagnosis of disease and differentiating between types of mammary tumors.

## V. REFERENCES


[1] F. L. Lizzi, M. Astor, T. Liu, C. Deng, D. J. Coleman, and R. H. Silverman, "Ultrasonic spectrum analysis for tissue assays and therapy evaluations," Int. J. Imaging Syst. Technol., **8**, 3-10 (1997).

[2] M. F. Insana, R. F. Wagner, D. G. Brown, and T. J. Hall, "Describing small-scale structure in random media using pulse-echo ultrasound," J. Acoust. Soc. Am., **87**, 179-192 (1990).

[3] M. L. Oelze, J. F. Zachary, and W. D. O'Brien Jr., "Characterization of tissue microstructure using ultrasonic backscatter: Theory and technique for optimization using a Gaussian form factor," J. Acoust. Soc. Am., 112, 1202-1211 (2002).

[4] M. F. Insana and T. J. Hall, "Parametric ultrasound imaging from backscatter coefficient measurements: image formation and interpretation," Ultrason Imaging, **12**, 245-267 (1990).

[5] J. A. Zagzebski, Z. F. Lu and L. X. Yao, "Quantitative ultrasound imaging: in vitro results in normal liver," Ultrason Imaging, **15**, 335-351 (1983).

[6] E. J. Feleppa, T. Liu, A. Kalisz, M. C. Shao, N. Fleshner and V. Reuter, "Ultrasonic spectral-parameter imaging of the prostate," Int. J. Imaging Syst. Technol., **8**, 11-25 (1997).

[7] D. Nicholas, "Evaluation of backscattering coefficients for excised human tissues: results, interpretation and associated measurements," Ultrasound Med. Biol., **8**, 17-28 (1982).

[8] D. K. Nassiri, and C. R. Hill, "The use of angular scattering measurements to estimate structural parameters of human and animal tissues," J. Acoust. Soc. Am., **87**, 179-192 (1990).

[9] G. A. Teotica, R. J. Miller, L. A. Frizzell, J. F. Zachary, and W. D. O'Brien, Jr., "Attenuation coefficient estimates of mouse and rat chest wall," IEEE Trans. Ultrason., Ferroelect., Freq. Cont., **48**, 593-600 (2001).